Tunable photonic band schemes in two-dimensional photonic crystals composed of copper oxide high-temperature superconductors

Hiroyuki Takeda and Katsumi Yoshino
Department of Electronic Engineering, Graduate School of Engineering, Osaka University, 2-1 Yamada-oka, Suita, Osaka 565-0871, Japan

(Received 15 October 2002; revised 18 December 2002; published 25 June 2003)

We theoretically demonstrate the tunability of two-dimensional photonic crystals composed of copper oxide high-temperature superconductors (HTSCs). The photonic crystals we deal with are composed of rods whose axes are parallel to the *c* axes in the copper oxide HTSC. Photonic crystals composed of copper oxide HTSCs exhibit the large tunabilities by temperature and magnetic fields. That is, a photonic band gap increases and a midgap frequency decreases with increasing temperature and the magnetic field. Their characteristics are due to the temperature dependence of London penetration depths and the magnetic field dependence of the critical temperature and the London penetration depths. The frequency range in which the photonic band gap appears are strongly dependent on materials in the copper oxide HTSCs.

DOI: 10.1103/PhysRevB.67.245109 PACS number(s): 42.70.Qs

I. INTRODUCTION

Recently, dielectric periodic structures of the order of optical wavelengths have attracted much attention as photonic crystals from theoretical and practical viewpoints, because concepts such as photonic band gaps have been predicted, and also various applications of photonic crystals have been proposed.[1–3] In earlier work, two optical principles, namely, the localization of light[4–6] and the controllable inhibition of spontaneous emission of light[7–10] were considered to be the most important. Photonic band schemes strongly depend on dielectric indices and structures of photonic crystals. Especially in the case of metals and semiconductors, photonic band schemes strongly depend on plasma frequencies.[11,12]

With respect to applications to optical devices, on the other hand, it is advantageous to obtain the tunability in photonic crystals. For example, we have proposed various voltage and temperature tunable photonic crystals composed of conducting polymers and liquid crystals infiltrated in silica opals and inverse opals, because refractive indices of conducting polymers and liquid crystals can be controlled by changing the temperature and applied voltages.[13,14] Moreover, it has been reported that it is possible to obtain tunable photonic crystals by the change of plasma frequencies in semiconductors under the influence of temperature and current injections.[12] The plasma frequencies in semiconductors depend on densities of electrons which can be changed under the influence of temperature and current injections. Therefore, it is important to apply controllable physical phenomena in solid states to tunable photonic crystals.

For example, the superconductivity is strongly influenced by temperature and the magnetic field. In the superconducting state, the electromagnetic wave can propagate only in the range of the London penetration depths of materials. In the normal conducting state, however, London penetration depths become infinite, that is, the electromagnetic field can propagate in the material without any limitations. Therefore, we can expect the large tunability in photonic crystals composed of superconductors due to the transition from the superconducting state to the normal conducting one.

Thus, we propose the use of superconductors in photonic crystals. As examples of superconductors, here, we deal with copper oxide high temperature superconductors (HTSCs). It has been reported that two-dimensional photonic crystals composed of HTSCs with large plasma frequencies possess almost flat photonic band states.[15] These photonic crystals are assumed to be two-dimensional arrays of air cylinders embedded by superconducting hosts. However, temperature and magnetic field tunabilities of these photonic crystals have not been discussed. Unlike conventional superconductors, copper oxide HTSCs have high transition temperature such as 30–150 [K]. Therefore, they are appropriate for applications, because some copper oxide HTSCs show the superconductivity under liquid nitrogen. However, we must consider that the construction of the lattice which contains copper oxide HTSCs is not generally easy, because the mechanical properties are so weak and that copper oxide HTSCs are so expensive. Copper oxide HTSCs have strong two-dimensional anisotropies, and the superconductivity appears in the two-dimensional anisotropic CuO planes. The *a* and *b* axes in copper oxide HTSCs are parallel to the two-dimensional anisotropic CuO plane, and the *c* axis is perpendicular to it. The electric fields parallel and perpendicular to the *c* axis feel different dielectric indices due to the strong two-dimensional anisotropy. The superconducting electrons are sensitive to the electric field perpendicular to the *c* axis rather than the electric field parallel to the *c* axis. At high frequencies, that is, the superconducting electrons are sensitive to the electric field perpendicular to the *c* axis. Therefore, plasma frequencies to the electric field parallel to the *c* axis are in the microwaves and far-infrared ranges that are much lower than those to electric field perpendicular to the *c* axis.[16]

In this paper, we theoretically investigate the tunability of two-dimensional photonic crystals composed of copper oxide HTSCs with square lattices. Rods which constitute

photonic crystals are assumed to be parallel to the c axis in copper oxide HTSCs. We deal with two kinds of copper oxide HTSCs: $Bi_{1.85}Pb_{0.35}Sr_2Ca_2Cu_{3.1}O_y$ and $Bi_2Sr_2CaCu_2O_{8+\delta}$.[17,18] We investigate the temperature and magnetic field tunability in photonic crystals composed of the former and the latter, respectively for the TM mode in which the electric field is parallel to the c axis ($E_z||c$).

II. THEORY

In order to determine photonic band schemes of photonic crystals composed of copper oxide HTSCs, we start with the wave equation satisfied by the electric field parallel to the z axis for two-dimensional periodic structures,

$$\frac{\partial^2 E_z(x,y)}{\partial x^2}+\frac{\partial^2 E_z(x,y)}{\partial y^2} = -\frac{\omega^2}{c^2}\epsilon(x,y)E_z(x,y)-i\mu_0\omega\{J_{sz}(x,y,\omega)+J_{nz}(x,y,\omega)\}, \tag{1}$$

where

$$J_{sz}(x,y,\omega)=n_s(x,y)(-e)v_{sz}(\omega) =n_s(x,y)(-e)\frac{e}{im\omega}E_z(x,y) =-\frac{n_s(x,y)e^2}{im\omega}E_z(x,y), \tag{2a}$$

$$J_{nz}(x,y,\omega)=n_n(x,y)(-e)v_{nz}(\omega) =n_n(x,y)(-e)\frac{e}{m(i\omega-\gamma)}E_z(x,y) =-\frac{n_n(x,y)e^2}{im(\omega+i\gamma)}E_z(x,y). \tag{2b}$$

$J_{sz}(x,y,\omega)$ and $J_{nz}(x,y,\omega)$ are superconducting and normal conducting electronic current densities to the z axis, $n_s(x,y)$ and $n_n(x,y)$ are superconducting and normal conducting electron densities and $v_{sz}(\omega)$ and $v_{nz}(\omega)$ are superconducting and normal conducting electron velocities parallel to the z axis, respectively in the two fluid model. $\epsilon(x,y)$ is a dielectric constant. γ is a damping term. From the phenomenological viewpoint, $v_{sz}(\omega)$ and $v_{nz}(\omega)$ are obtained by the equation of motion of electrons.

Substituting Eqs. (2a) and (2b) into Eq. (1) results in the following wave equation:

$$\begin{aligned}\frac{\partial^2 E_z(x,y)}{\partial x^2}+\frac{\partial^2 E_z(x,y)}{\partial y^2} &= -\frac{\omega^2}{c^2}\left\{\epsilon(x,y)-\frac{\mu_0 n_s(x,y)e^2c^2/m}{\omega^2} -\frac{n_n(x,y)e^2/m\epsilon_0}{\omega(\omega+i\gamma)}\right\}E_z(x,y)\\ &= -\frac{\omega^2}{c^2}\left\{\epsilon(x,y)-\frac{c^2/\lambda(x,y)^2}{\omega^2} -\frac{n_n(x,y)e^2/m\epsilon_0}{\omega(\omega+i\gamma)}\right\}E_z(x,y)\\ &= -\frac{\omega^2}{c^2}\epsilon(x,y)\left\{1-\frac{\omega_{sp}(x,y)^2}{\omega^2} -\frac{\omega_{np}(x,y)^2}{\omega(\omega+i\gamma)}\right\}E_z(x,y),\end{aligned} \tag{3}$$

where $\lambda(x,y)=\sqrt{m/\mu_0 n_s(x,y)e^2}$,

$$\omega_{sp}(x,y)=c/\lambda(x,y)\sqrt{\epsilon(x,y)}$$

and

$$\omega_{np}(x,y)=\sqrt{n_n(x,y)e^2/m\epsilon_0\epsilon(x,y)}.$$

$\lambda(x,y)$, $\omega_{sp}(x,y)$ and $\omega_{np}(x,y)$ are the London penetration depth and the plasma frequencies of superconducting and normal conducting electrons, respectively. $\omega_{sp}(x,y)$ strongly depends on the London penetration depth. Indeed, the density of the superconducting electrons decreases with depth exponentially within the rods. In the experiments[17,18]; however, plasma frequencies are observed without the consideration of dependences of the superconducting electrons on depth. In this paper, therefore, plasma frequencies are assumed to be uniform within the rods, for simplicity. From Eq. (3), the effective dielectric index $\epsilon_{eff}(x,y,\omega)$ is represented as follows:

$$\epsilon_{eff}(x,y,\omega)=\epsilon(x,y)\left\{1-\frac{\omega_{sp}(x,y)^2}{\omega^2}-\frac{\omega_{np}(x,y)^2}{\omega(\omega+i\gamma)}\right\}. \tag{4}$$

As shown in Eq. (4), $\epsilon_{eff}(x,y,\omega)$ depends on $\omega_{sp}(x,y)$ and $\omega_{np}(x,y)$. In the frequency range we consider below, however, $\omega_{np}(x,y)^2/\omega(\omega+i\gamma)$ does not affect $\epsilon_{eff}(x,y,\omega)$ much.[17,18] Therefore, we neglect the third term on the right side of Eq. (4), and then $\epsilon_{eff}(x,y,\omega)$ becomes a simple Drude model. Metallic photonic crystals are also described by the Drude model. They have cutoff frequencies due to plasma frequencies in the TM mode, and band structures in the TM mode significantly differ from those in the TE mode.[19] Moreover, there are interesting reports about metallic photonic crystals.[20,21]

In Fig. 1, we show a rod composed of copper oxide HTSCs. The a, b, and c axes are defined as shown in this figure. The rod is parallel to the c axis. We evaluate for the TM mode in two-dimensional photonic crystals, that is, the

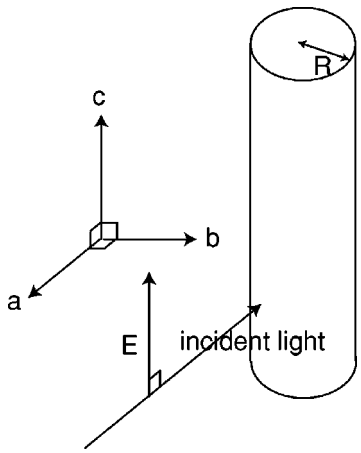

FIG. 1. Structure of a rod composed of copper oxide HTSCs and *a*, *b*, and *c* axes. The *a* and *b* axes are parallel to the two-dimensional anisotropic plane, and the *c* axis is perpendicular to the two-dimensional anisotropic plane. The rod and the electric field are parallel to the *c* axis ($\mathbf{E}||\mathbf{c}$).

electric field is parallel to the *c* axis ($E_z||c$). As mentioned earlier, we must clarify the polarized vector of the electric field, because copper oxide HTSCs have the strong two-dimensional anisotropy.

The effective dielectric index $\epsilon_{eff}(x+R_x,y+R_y)=\epsilon_{eff}(x,y)$ is periodic with respect to the lattice vector $R_{x,y}$ generated by the primitive translation and it may be expanded in a Fourier series on $G_{x,y}$, the reciprocal lattice vector

$$\epsilon_{eff}(x,y,\omega)=\sum_{G_x,G_y}\epsilon_{eff}(G_x,G_y,\omega)\exp\{i(G_x x+G_y y)\}. \tag{5}$$

Using Bloch's theorem, we may expand the electric field as

$$E_z(x,y)=\sum_{G_x,G_y}E_z(G_x,G_y)\exp[i\{(k_x+G_x)x+(k_y+G_y)y\}], \tag{6}$$

where $k_{x,y}$ is the wave vector. The right side of Eq. (3) is separated into a first term dependent on frequencies and a second term independent of frequencies. By inserting Eqs. (5) and (6) into Eq. (3), we obtain the matrix eigenvalue problem with respect to frequencies. Therefore, photonic band structures of the copper oxide HTSCs can be obtained by solving frequencies at a certain wave vector. A more detailed explanation is given in Ref. 12.

III. NUMERICAL CALCULATION AND DISCUSSION

First, we investigate the temperature tunability of two-dimensional photonic crystals composed of copper oxide HTSCs with square lattices. We deal with $Bi_{1.85}Pb_{0.35}Sr_2Ca_2Cu_{3.1}O_y$ as copper oxide HTSCs.[17] We suppose that the dielectric index is $\epsilon=12$, the lattice constant is $a=250$ [μm] and the radius of the rod is $R/a=0.2$. A background of the photonic crystal is air. At 5 [K], the London penetration depth is $\lambda(5[K])=23$ [μm], which corresponds to $\omega_{sp}(5[K])=3.77$ [THz] ($\omega_{sp}(5$ [K]$)a/2\pi c=0.5$). That is, here our attention is focused on the far-infrared region. In experimental studies,[17] plasma frequencies are not observed in such a frequency region at the normal conducting state, which means that the third term on the right side of Eq. (4) can be neglected in such a frequency region.

Photonic band schemes evaluated at $T=5$ [K] (below $T_c=107$ [K]) and at $T\geqslant T_c=107$ [K] are shown in Figs. 2(a) and 2(b), respectively. Shaded regions in these figures indicate photonic band gaps. It should be noted that the photonic band scheme in Fig. 2(a) significantly differs from that in Fig. 2(b). In Fig. 2(a), a photonic band gap exists at $\omega a/2\pi c\leqslant 0.339$, that is, a cutoff frequency exists. This is because the plasma frequency exists, and therefore, the light only in the frequency range $\omega a/2\pi c\geqslant\omega_{cutoff}a/2\pi c=0.339$ can propagate in the photonic crystal. Moreover, it should be noted that $\omega_{cutoff}a/2\pi c$ is lower than $\omega_{sp}a/2\pi c$. That is, plasma frequencies in uniform media are different from those in photonic crystals.[19]

As shown in Fig. 2(b), on the other hand, the photonic band scheme at temperatures above T_c is very different. This is because ω_{sp} becomes zero at temperature higher than the transition temperature T_c. Thus, cutoff frequencies decrease

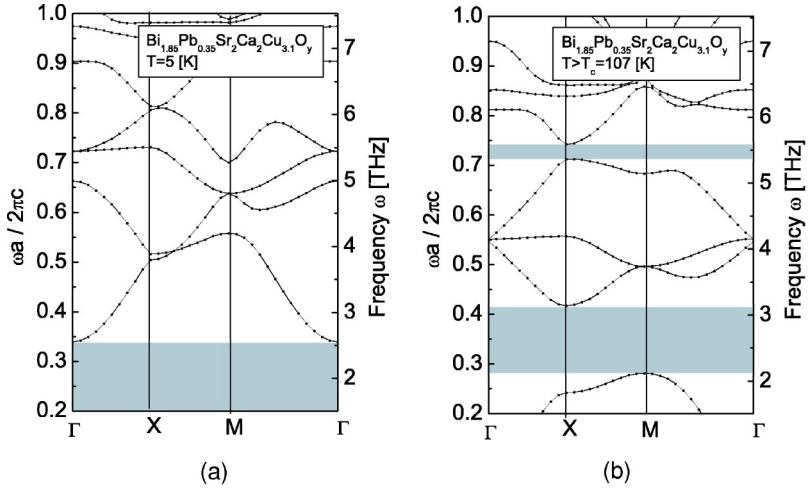

FIG. 2. Photonic band schemes of two-dimensional photonic crystals composed of copper oxide HTSCs (a) at $T=5$ [K] and (b) at $T\geqslant T_c=107$ [K].

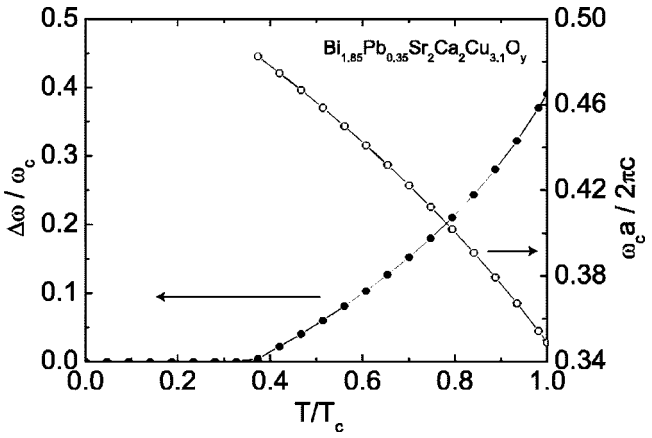

FIG. 3. Dependences of the photonic band gap per midgap ratio and the midgap on temperature. Black and white points indicate the photonic band gap per midgap ratio and the midgap, respectively.

monotonically with increasing temperature. As shown in Fig. 2(b), however, another photonic band gaps appear at higher frequencies. That is, the large tunability can be realized in two-dimensional photonic crystals due to the transition from the superconducting state to the normal conducting one under the influence of temperature.

In copper oxide HTSCs, the following dependence of the London penetration depth on temperature is known:

$$\lambda(T \leqslant T_c) = \lambda(0\ \ [\mathrm{K}])/\sqrt{1-T/T_c}. \tag{7}$$

We can obtain valuable information for the change of temperature, although Eq. (7) is not an exact relation. Then, the dependence of the plasma frequency on temperature is given as follows from Eq. (7):

$$\omega_{sp}(T \leqslant T_c) = \omega_{sp}(0\ \ [\mathrm{K}])\sqrt{1-T/T_c}. \tag{8}$$

In the frequency region $\omega \geqslant \omega_{cutoff}$, we focus our attention on a band gap which appears in the frequency of $(0.2\text{-}0.5)2\pi c/a$ with increasing temperature. Dependences of the band gap per midgap ratio and the midgap on temperature are shown in Fig. 3. Black and white points indicate the band gap per midgap ratio and the midgap, respectively. Around $T/T_c = 0.4$, the band gap appears and increases monotonically with increasing temperature. On the other hand, the midgap decreases monotonically with increasing temperature. That is, we can control opening and closing band gaps under the influence of temperature in the far infrared region.

Next, the magnetic field tunability of two-dimensional photonic crystals composed of copper oxide HTSCs with square lattices is investigated. Here we treat with $Bi_2Sr_2CaCu_2O_{8+\delta}$ as copper oxide HTSCs.[18] The transition temperature T_c of the material is 85 [K]. We suppose that the dielectric index is $\epsilon = 10$, the lattice constant is $a = 10$ [mm] and the radius of the rod is $R/a = 0.2$. A background of the photonic crystal is air.

In the superconducting state at 55 [K] under the magnetic field applied parallel to the c axis in the photonic crystal $(E_z||B_z||\mathrm{c})$, the plasma frequency ω_{sp} satisfies the following relation in the magnetic field region of 0.1–1 [T] (Ref. 18):

$$\omega_{sp}(0.1[T] \leqslant B \leqslant 1[T] < B_c) = \frac{30}{\sqrt{B}}\ [\mathrm{GHz}]. \tag{9}$$

That is, we focus our attention on the microwave region. The damping constant γ of this superconductor is about 1 [THz], which is much larger than the microwave frequency. Therefore, we can neglect the third term on the right side of Eq. (4) in such a frequency region.[18] The dependence of ω_{sp} on the magnetic field results from the phase difference between the CuO planes and the nature of vortex decoupling.

Photonic band schemes at $B = 0.1$ [T] and at $B \geqslant B_c$ are indicated in Figs. 4(a) and 4(b), respectively. Shaded regions indicate photonic band gaps. It should be noted that the photonic band scheme in Fig. 4(a) significantly differs from that in Fig. 4(b). At $B = 0.1$ [T], $\omega_{sp}(0.1\ [\mathrm{T}]) = 94.87$ [GHz] $(\omega_{sp}a/2\pi c = 0.5)$. In Fig. 4(a), the photonic band gap exists at $\omega a/2\pi c \leqslant 0.329$, that is, a cutoff frequency exists. This is because the plasma frequency exists, and therefore, the light only in the frequency range $\omega a/2\pi c \geqslant \omega_{cutoff}a/2\pi c = 0.329$ can propagate in the photonic crystals. For the case shown in Fig. 4(b), on the other hand, ω_{sp} becomes zero, because the magnetic field is larger than the critical magnetic field B_c. Thus, cutoff frequencies decrease monotonically with in-

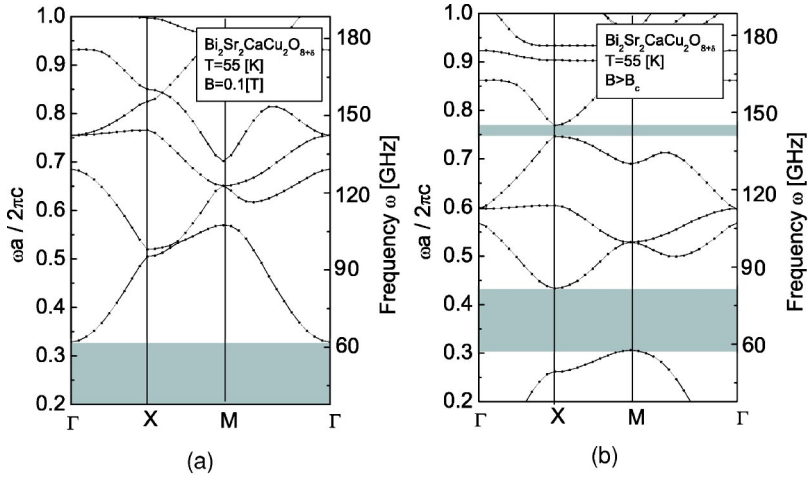

FIG. 4. Photonic band schemes of two-dimensional photonic crystals composed of copper oxide HTSCs (a) at $B = 0.1$ [T] and (b) at $B \geqslant B_c$ at $T = 55$ [K].

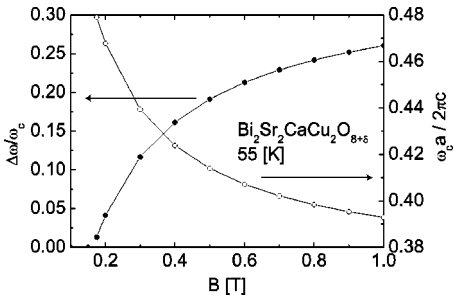

FIG. 5. Dependences of the photonic band gap per midgap ratio and the midgap on the magnetic field when the magnetic field is applied to the c axis ($\mathbf{E}||\mathbf{B}||\mathbf{c}$). Black and white points indicate the photonic band gap per midgap ratio and the midgap, respectively.

creasing the magnetic field. As shown in Fig. 4(b), however, another photonic band gap appears. Therefore, the large tunability can be realized in two-dimensional photonic crystals due to the change from the superconducting state to the normal conducting one upon applications of the magnetic field.

In the frequency region $\omega \geqslant \omega_{cutoff}$, we focus our attention on the band gap which appears in the frequency of $(0.2\text{-}0.5)2\pi c/a$ with increasing the magnetic field. In Fig. 5, dependences of the band gap per midgap ratio and the midgap on the applied magnetic field are shown. Black and white points indicate the band gap per midgap ratio and the midgap, respectively. Around $B=0.15$ [T], the band gap appears and increases monotonically with increasing the magnetic field. On the other hand, the midgap decreases monotonically with increasing magnetic field. Although the critical magnetic field is not given in Ref. 18, ω_{sp} becomes zero at $B \geqslant B_c$. At $B \geqslant B_c$, $\Delta\omega/\omega_c = 0.344$ and $\omega_c a/2\pi c = 0.370$. That is, we can control opening and closing band gaps under the influence of the magnetic field in the microwave region.

Moreover, we investigate dependences of the band gap per midgap ratio and the midgap on temperature at the constant magnetic field. At $0.3 \leqslant T/T_c \leqslant 0.7$ and $0.1\ [\mathrm{T}] \leqslant B \leqslant 1\ [\mathrm{T}]$, $\omega_{sp}(T,B)$ is represented as follows.[18]

$$\omega_{sp}(0.3T_c \leqslant T \leqslant 0.7T_c, 0.1\ [\mathrm{T}] \leqslant B \leqslant 1\ [\mathrm{T}]) = \frac{222.5}{\sqrt{BT}}\ [\mathrm{GHz}]. \tag{10}$$

This equation coincides with Eq. (9) at $T=55$ [K]. In Fig. 6, we show dependences of the band gap per midgap ratio and the midgap on temperature ranging from $0.3T_c$ to $0.7T_c$ at $B=0.6$ [T]. The band gap increases and the midgap decreases monotonically with increasing temperature. However, these behaviors are different from those in Fig. 3. That is, the temperature tunability of two-dimensional photonic crystals composed of copper oxide HTSCs with square lattices are affected by the existence of the magnetic field.

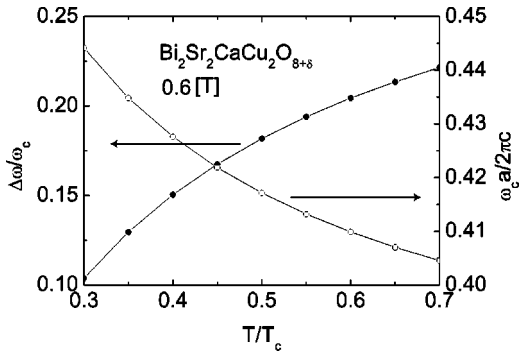

FIG. 6. Dependences of the photonic band gap per midgap ratio and the midgap on temperature ranging from $0.3T_c$ to $0.7T_c$ at $B=0.6$ [T]. Black and white points indicate the photonic band gap per midgap ratio and the midgap, respectively.

As evident by the comparison of Figs. 2 and 4, the frequency region in which photonic band gaps appear is strongly dependent on materials in copper oxide HTSCs. In the present case, the photonic band gaps appear in the far infrared region in $Bi_{1.85}Pb_{0.35}Sr_2Ca_2Cu_{3.1}O_y$ and in the microwave region in $Bi_2Sr_2CaCu_2O_{8+\delta}$. These results may provide novel application to tunable photonic crystals. As shown in Figs. 3, 5 and 6, for example, $\omega_c a/2\pi c$ can be changed by temperature and the magnetic field, which means that reflective peak frequencies can be controlled by the external factors. Moreover, the flow of light can also be controlled by opening and closing photonic band gaps.

IV. CONCLUSION

In conclusion, we theoretically demonstrated the tunability of two-dimensional photonic crystals composed of copper oxide HTSCs. The photonic crystals we deal with are composed of rods whose axes are parallel to the c axes in the copper oxide HTSC. Photonic crystals composed of copper oxide HTSCs exhibit the large tunabilities by temperature and magnetic fields. That is, a photonic band gap increases and a midgap frequency decreases with increasing temperature and magnetic fields. Their characteristics are due to the temperature dependence of London penetration depths and the magnetic field dependence of the critical temperature and the London penetration depths. The frequency range in which the photonic band gap appears are strongly dependent on materials in copper oxide HTSCs.

ACKNOWLEDGMENT

This work was partly supported by a Grant-in-Aid for Scientific Research from the Ministry of Education, Culture, Sports, Science and Technology (Grant No. 14205046) and from the Japan Society for the Promotion of Science.

[1] S. John, Phys. Rev. Lett. **58**, 2486 (1987).
[2] E. Yablonovitch, Phys. Rev. Lett. **58**, 2059 (1987).
[3] S. John and T. Quang, Phys. Rev. Lett. **74**, 3419 (1995).
[4] S. John, Phys. Rev. Lett. **53**, 2169 (1984).
[5] A.Z. Genack and N. Garcia, Phys. Rev. Lett. **66**, 2064 (1991).
[6] D. Wiersma, P. Bartolini, A. Lagendijk, and R. Righini, Nature (London) **390**, 671 (1997).
[7] V.P. Bykov, Sov. J. Quantum Electron. **4**, 861 (1975).
[8] S. John and J. Wang, Phys. Rev. Lett. **64**, 2418 (1990).
[9] S. John and T. Quang, Phys. Rev. A **50**, 1764 (1994).
[10] T. Quang, M. Woldeyohannes, S. John, and G.S. Agarwal, Phys. Rev. Lett. **79**, 5238 (1997).
[11] S. Fan, P.R. Villeneuve, and J.D. Joannopoulos, Phys. Rev. B **54**, 11 245 (1996).
[12] P. Halevi and F. Ramos-Mendieta, Phys. Rev. Lett. **85**, 1875 (2000).
[13] K. Yoshino, S. Satoh, Y. Shimoda, Y. Kawagishi, K. Nakayama, and M. Ozaki, Jpn. J. Appl. Phys., Part 2 **38**, L961 (1999).
[14] K. Yoshino, Y. Shimoda, Y. Kawagishi, K. Nakayama, and M. Ozaki, Appl. Phys. Lett. **75**, 932 (1999).
[15] W.M. Lee, P.M. Hui, and D. Stroud, Phys. Rev. B **51**, 8634 (1995).
[16] Y. Zha, K. Levin, and D.Z. Liu, Phys. Rev. B **51**, 6602 (1995).
[17] H. Shibata and T. Yamada, Phys. Rev. B **54**, 7500 (1996).
[18] Y. Matsuda, M.B. Gaifullin, K. Kumagai, K. Kadowaki, and T. Mochiku, Phys. Rev. Lett. **75**, 4512 (1995).
[19] V. Kuzmiak, A.A. Maradudin, and F. Pincemin, Phys. Rev. B **50**, 16 835 (1994).
[20] J.M. Pitarke, F.J. Garcia-Vidal, and J.B. Pendry, Phys. Rev. B **57**, 15 261 (1998).
[21] M.I. Antonoyiannakis and J.B. Pendry, Phys. Rev. B **60**, 2363 (1999).